2902 J. Med. Chem. 2010, 53, 2902–2912
DOI: 10.1021/jm901532h

Journal of Medicinal Chemistry Article

3′-[4-Aryl-(1,2,3-triazol-1-yl)]-3′-deoxythymidine Analogues as Potent and Selective Inhibitors of Human Mitochondrial Thymidine Kinase

Sara Van Poecke,[†] Ana Negri,[‡] Federico Gago,[‡] Ineke Van Daele,[†] Nicola Solaroli,[§] Anna Karlsson,[§] Jan Balzarini,[∥] and Serge Van Calenbergh*,[†]

[†]*Laboratory for Medicinal Chemistry (FFW), Ghent University, Harelbekestraat 72, 9000 Gent, Belgium,* [‡]*Departamento de Farmacologia, Universidad de Alcalá, E-28871 Alcalá de Henares, Madrid, Spain,* [§]*Karolinska Institute, S-14157 Stockholm, Sweden, and* [∥]*Rega Institute for Medical Research, Katholieke Universiteit Leuven, B-3000 Leuven, Belgium*

Received October 16, 2009

In an effort to increase the potency and selectivity of earlier identified substrate-based inhibitors of mitochondrial thymidine kinase 2 (TK-2), we now describe the synthesis of new thymidine analogues containing a 4- or 5-substituted 1,2,3-triazol-1-yl substituent at the 3′-position of the 2′-deoxyribofuranosyl ring. These analogues were prepared by Cu- and Ru-catalyzed cycloadditions of 3′-azido-3′-deoxythymidine and the appropriate alkynes, which produced the 1,4- and 1,5-triazoles, respectively. Selected analogues showed nanomolar inhibitory activity for TK-2, while virtually not affecting the TK-1 counterpart. Enzyme kinetics indicated a competitive and uncompetitive inhibition profile against thymidine and the cosubstrate ATP, respectively. This behavior is rationalized by suggesting that the inhibitors occupy the substrate-binding site in a TK-2−ATP complex that maintains the enzyme's active site in a closed conformation through the stabilization of a small lid domain.

Introduction

In mammalian cells, four different deoxynucleoside kinases can be found: thymidine (dThd) kinase 1 (TK-1[a]), thymidine kinase 2 (TK-2), deoxycytidine kinase (dCK), and deoxyguanosine kinase (dGK). The main role of these kinases is to convert deoxynucleosides to their monophosphates by γ-phosphoryl transfer of ATP, an essential step in the biosynthesis of the DNA building blocks. A second fundamental role lies in the activation of nucleoside analogues with pharmacological (anticancer and antiviral) properties.

Among these mammalian deoxynucleoside kinases, two enzymes phosphorylate thymidine (dThd), TK-1 and TK-2. The main differences between these two kinases with respect to amino acid sequences, substrate specificities, localization, and levels of expression during the different cell cycle phases are summarized in Table 1.[1,2] Mitochondrial DNA (mtDNA) replication takes place throughout the whole cell cycle, thus constantly requiring deoxynucleoside triphosphates for mtDNA synthesis. By being active in nonproliferating tissues, TK-2 provides the nucleotides for mtDNA synthesis. Consequently, TK-2 deficiency leads to mitochondrial disorders, designated as mtDNA depletion syndromes, mostly affecting skeletal muscles.[3]

Besides the mitochondrial disorders linked to TK-2 deficiency, severe mitochondrial toxicity is also associated to long-term treatment with antiviral nucleoside analogues such as AZT.[4,5] Although the mechanism by which these nucleoside analogues exert their mitochondrial toxicity is not fully understood, it has been suggested that after phosphorylation of the nucleoside analogues by TK-2, their triphosphates accumulate in the mitochondria. In the case of AZT, phosphorylation in nonreplicating cells by TK-2 is significant, despite the fact that it is not an ideal substrate for TK-2. The accumulation of AZT-TP is suggested to affect DNA-polymerase-γ, resulting in mtDNA depletion.[4]

Likewise, mitochondrial toxicity is a major concern in the development of new nucleoside drugs, as exemplified back in 1993 by the halting of a clinical trial of fialuridine (FIAU) because patients developed serious liver and kidney toxicity, later found to originate from incorporation of the drug into mitochondrial DNA.

TK-2 inhibitors can be a valuable tool to answer the many open questions regarding the real contribution of TK-2 in the maintenance and homeostasis of mitochondrial dNTP pools and to clarify the role of this enzyme in the mitochondrial toxicity of a variety of antiviral and anticancer drugs.

Despite the lack of a crystal structure of TK-2 for structure-based inhibitor design, several TK-2 inhibitors have been identified in the past (Chart 1). A noteworthy example is the ribonucleoside 5-(*E*)-(2-bromovinyl)uridine (**1**; $K_i = 10.4\ \mu M$), whose 2′-deoxy congener is an alternative substrate for the enzyme.[6] Another study describes nucleosides modified at the sugar moiety, including 3′-*O*-alkyl analogues and 3′-hexanoylamino-3′-deoxythymidine **2**, a very potent inhibitor of TK-2 ($K_i = 0.15\ \mu M$).[7] While 1-β-D-arabinofuranosylthymine (AraT) and (*E*)-5-(2-bromovinyl)-1-β-D-arabinofuranosyluracil (BVaraU) represent good substrates for TK-2, the introduction of long chain acyl substituents at the 2′-OH (as in **3**; $IC_{50} = 6.3\ \mu M$) turned these substrates into potent inhibitors. Unfortunately, these 2′-*O*-acyl derivatives cannot be used as tools to study TK-2 in intact cells because they are unstable in cell culture and readily converted to the parent nucleoside.[8]

*To whom correspondence should be addressed. Phone: +32 9 264 81 24. Fax: + 32 9 264 81 46. E-mail: serge.vancalenbergh@ugent.be.

[a]Abbreviations: TK, thymidine kinase; HSV, herpes simplex virus; VZV, varicella zoster virus; Dm, *Drosophila melanogaster*; dNK, deoxynucleoside kinase; dThd, thymidine; AZT, azidothymidine.

 Published on Web 03/10/2010 © 2010 American Chemical Society

Table 1. The Most Important Features of TK-1 and TK-2

	TK-1	TK-2
amino acid sequence	unique in its group	belongs to a larger group of nucleosides: similar to dCK, dGK, Dm-dNK[a] (40% sequence homology), HSV-1
substrate specificity:		
natural nucleosides	thymidine, 2′-deoxyuridine	thymidine, 2′-deoxyuridine, 2′-deoxycytidine
antiviral nucleoside analogues	AZT: excellent substrate	AZT: poor substrate, but in nondividing cells TK-2 phosphorylation becomes significant.
	Ara-T: weak substrate	Ara-T: good substrate
localization	cytosol	mitochondria
levels of expression	highest expression in S phase cells; very low activity in resting cells	constitutively expressed, physiologically active in nonproliferating and resting cells.

[a] Dm dNK: multisubstrate deoxynucleoside kinase of the fruit fly *Drosophila melanogaster*. [b] HSV-1 TK: thymidine kinase of *Herpes simplex* virus type 1.

Chart 1. Structures of Reported TK-2 Inhibitors

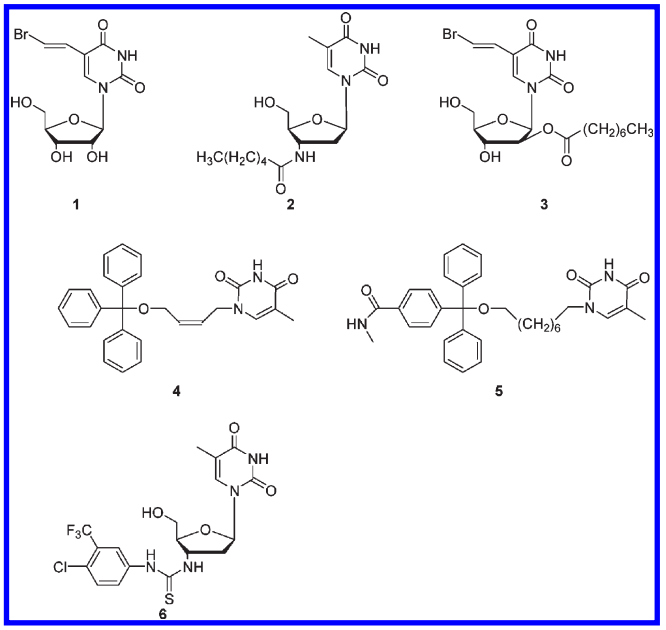

After the identification of 5′-*O*-trityl-thymidine as a moderately active inhibitor of TK-2 ($IC_{50} = 33\ \mu M$), Pérez-Peréz et al. replaced the sugar moiety of this nucleoside by acyclic spacers to tether the thymine base to a distal triphenylmethoxy moiety.[9] Elaborate optimization of the TK-2 inhibitory activity of 1-[(*Z*)-4-(triphenylmethoxy)-2-butenyl]thymine **4** ($IC_{50} = 1.5\ \mu M$) yielded the acyclic analogue **5** with an IC_{50} value of $0.4\ \mu M$.[10]

Recently, we evaluated two series of thymidine analogues, which had been originally designed as *Mycobacterium tuberculosis* thymidylate kinase inhibitors, for their inhibitory activity against a panel of other nucleoside kinases (TK-1, TK-2, HSV-1 TK, and VZV TK).[11] Several substituted 3′-thiourea derivatives of β-dThd proved highly inhibitory to and selective for human mitochondrial TK-2 compared to the other enzymes. Compound **6**, which emerged as the most potent analogue of this series, inhibited TK-2 at concentrations 2100-fold lower than those required to inhibit cytosolic TK-1 (IC_{50}: TK-1, 316 μM; TK-2, 0.15 μM). Kinetic experiments indicated that this inhibitor specifically binds to the enzyme−ATP complex, and in consonance with this finding molecular modeling studies suggested that the nitrogen atoms of the thiourea group of **6** could interact favorably with the oxygens of the γ-phosphate of the cosubstrate ATP.

As it was demonstrated that the 3′-substituent of **6** and related analogues was responsible for extra interactions with TK-2 (after binding of the ATP phosphoryl donor), we decided to investigate if the thiourea moiety, earlier described as the perpetrator of toxicity,[12] could be replaced by alternative linkages to connect the C-3′ atom of the deoxyribose moiety to several substituents. In this study, we explore thymidine analogues containing a triazole ring instead of the thiourea moiety.

The discovery that a Cu(I)-catalyzed 1,3-dipolar cycloaddition reaction between azides and alkynes efficiently and regioselectively forms 1,4-substituted 1,2,3-triazoles, reported as the first "click chemistry" reaction,[13] boosted its application for lead identification and lead optimization procedures in drug discovery.[14] This Huisgen−Sharpless cycloaddition has also proven useful in the nucleoside/nucleotide field for the construction of different bioconjugates,[15] modified bases,[16] sugar residues,[17] and altered phosphodiester backbones,[18] as recently reviewed by Schinazi et al.[19]

Because of its synthetic convenience and the accessibility of AZT as the azide precursor, we decided to apply the click reaction to synthesize a series of 3′-(1,2,3-triazol-1-yl) analogues of dThd. In addition, a triazole is relatively resistant to metabolic degradation[20] and has a high dipole moment (about 5 D),[21] which, we believed, could favor its interaction with the γ-phosphate group of ATP.

It should be noted that, in search for new antivirals resembling AZT, Wigerinck et al. already reported 3′-triazole thymidine analogues in 1989.[22] However, at that time, these were obtained by classical (thermal) Huisgen reaction conditions[23] (i.e., in the absence of a Cu^+ catalyst), which generally resulted in mixtures of the 1,4- and the 1,5-regioisomers that are not always easy to separate by classical chromatographic procedures.

As a further extension of this study, we also wanted to explore the effect of analogues that combined a favorable 3′-(4-substituted-1,2,3-triazole) moiety with a (*E*)-5-(2-bromovinyl)-substituent, known as a privileged scaffold for TK-2 binding.

Results and Discussion

Chemistry. AZT (**7**) was converted into the 1,4-disubstituted 1,2,3-triazoles **8a**−**h** through Huisgen−Sharpless 1,3-dipolar cycloadditions with the appropriate alkynes in the presence of copper(II) sulfate and sodium ascorbate (Scheme 1). The isomeric 1,5-disubstituted 1,2,3-triazoles **8i**−**j** were obtained in moderate yields upon reaction of AZT with the appropriate alkynes in the presence of $[Cp^*RuClP(Ph_3)_2]$.[24]

Unambiguous assignment of the substitution pattern of the triazole moiety of isomers **8c** and **8i** could be inferred from comparison of their ^{13}C NMR spectra with that of the monosubstituted triazole **8a** (Table 2). In the case of **8c**, the largest resonance shift is found for the C-4″ (13.0 ppm), while the shift for C-5″ is relatively weak and has the sign changed (−3.5 ppm). An opposite phenomenon is observed for **8i**, where these shifts are 4.7 ppm for C-4″ and 8.7 ppm for C-5″. The observed downfield shifts of the substituted carbon atoms is expected given the electron withdrawing nature of the phenyl ring.

The synthesis of the 5-(*E*)-(2-bromovinyl) analogues is depicted in Scheme 2. After 5′-*O* tritylation of BVDU (**9**), the corresponding 2,3′-anhydro intermediate **11** was prepared by consecutive mesylation and treatment of the mesylate with Et_3N in EtOH. Treatment of **11** with sodium azide and detritylation afforded the azido derivative **13**, which was converted to the 1,4-triazoles **14a**−**b** under "click" conditions.

Biological Evaluation. The 3′-triazole-substituted dThd derivatives were evaluated for their inhibitory activity against dThd phosphorylation by recombinant purified human cytosolic TK-1, human mitochondrial TK-2, HSV-1 TK, varicella-zoster virus (VZV) TK, and Dm dNK (Table 3). Compound **6**, the most potent TK-2 inhibitor reported to date, was included as a reference.

In the 1,4-triazole series, the anti-TK-2 activity was clearly influenced by the nature of the substituent at C-4 of the triazole. Both a *n*-butyl (**8b**) or phenyl (**8c**) substituent gave submicromolar inhibition. Introduction of a $-CH_2-$ group between the triazole and the phenyl (**8d**) did not drastically alter the IC_{50}, while replacement of the benzyl by a cyclopentylmethyl substituent (**8e**) caused a 2-fold drop in IC_{50}. Introduction of an electron-withdrawing Cl in the para position of the phenyl (**8f**) significantly improved the inhibitory activity. A similar effect had previously been observed in the thiourea series.[11] Remarkably, this increased activity could not be obtained with an electron-deficient pyridin-2-yl substituent (**8h**). With analogues **8i** and **8j**, which are regioisomers of **8c** and **8f**, we could infer that the 4-position is the preferred site for triazole derivatization.

Introduction of an additional 5-(2-bromovinyl) group, known to be a privileged substituent for TK-2 binding, only slightly improved the inhibitory activity but caused a significant increase in the selectivity for TK-2 versus TK-1 as seen from the complete lack of inhibitory effect against TK-1-catalyzed dThd phosphorylation. Compound **14b** showed an outstanding selectivity against TK-2 when compared to TK-1 (SI ≥ 14000), and also is, to our knowledge, the most potent inhibitor of TK-2 reported so far, with an IC_{50} of 0.036 μM. Because the K_m values of the natural substrate dThd for TK-1 (2.3 μM) and TK-2 (1.1 μM) were very similar and the IC_{50} values of the inhibitors were determined in the presence of 1 μM dThd, the IC_{50} values of the different inhibitors fairly reflect the degree of affinity of these compounds for both enzymes. In addition, **14b** showed relatively poor inhibitory activity against the closely related HSV-1 and VZV TKs.

The mode of TK-2 inhibition by **14b** was investigated (Figure 1). First, its K_i value was determined in the presence of a fixed saturating concentration of ATP and variable concentrations of the dThd substrate. This revealed that **14b** inhibited the enzyme in a purely competitive fashion and had K_i values as low as 0.012 μM. Its K_i/K_m ratios were markedly

Scheme 1[a]

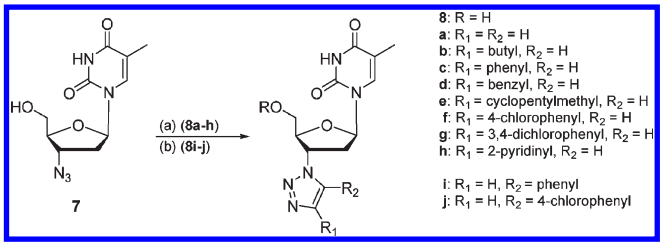

[a] Reagents and conditions: (a) appropriate alkyne, $CuSO_4 \cdot 5H_2O$, sodium ascorbate, H_2O/*t*-BuOH 1:1, rt, 24 h, 14−69%; (b) appropriate alkyne, Cp*RuCl(PPh_3)$_2$, THF, 65 °C, 8 h, 20−29%.

Table 2. ^{13}C-NMR Data of the Triazole Moieties of **8a**, **8c**, and **8i**

	C-4″	C-5″
8a	133.57	124.49
8c	146.57	121.01
8i	138.22	133.16

Scheme 2[a]

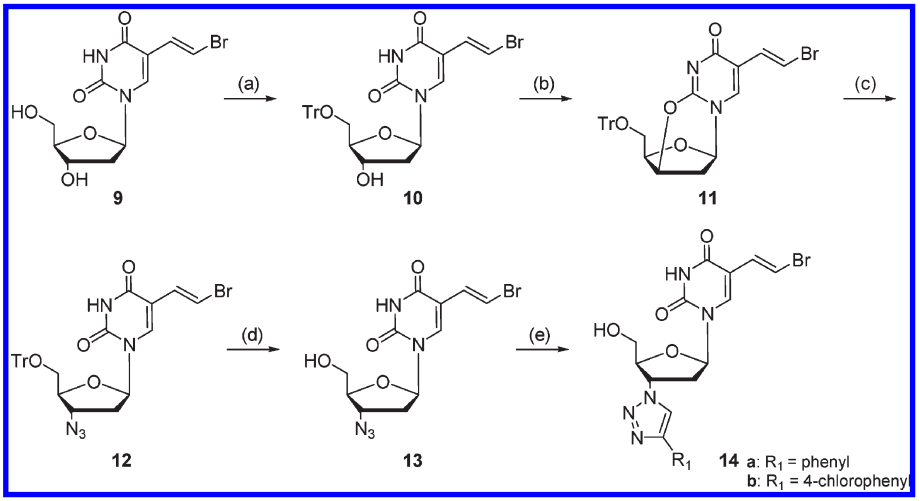

[a] Reagents and conditions: (a) TrCl, DMAP, pyridine, 65 °C, overnight, 65%; (b) (i) MsCl, pyridine, −78 °C → 0 °C, 4 h; (ii) Et_3N, EtOH, reflux, overnight, 75% over 2 steps; (c) NaN_3, 4-NO_2-phenol, DMF, 110 °C, overnight, 79%; (d) $ZnBr_2$, CH_2Cl_2/*i*PrOH 85:15, rt, overnight, 90%; (e) appropriate alkyne, $CuSO_4 \cdot 5H_2O$, sodium ascorbate, H_2O/*t*-BuOH 1:1, rt, 24 h, 6%.

Table 3. Inhibitory Activity of 3′-Triazol-1-yl Derivatives of Thymidine against Nucleoside Kinase-Catalysed Phosphorylation of 1 μM [CH_3-^{3}H]-Thymidine Compared with Thiourea **6**

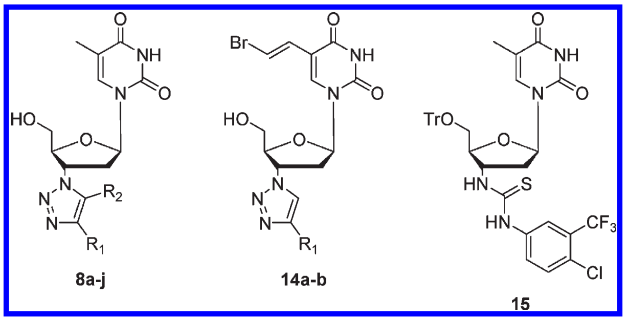

			IC_{50}[a] (μM)				
	R_1	R_2	TK-1	TK-2	HSV-1 TK	VZV TK	Dm dNK
8a	H	H	≥500	4.7 ± 2.1	212 ± 17	15 ± 5	40 ± 1
8b	*n*-Bu	H	366 ± 4	0.23 ± 0.05	95 ± 1	4.3 ± 0.3	4.1 ± 0.8
8c	Ph	H	54 ± 16	0.32 ± 0.01	28 ± 6	2.5 ± 0.3	2.2 ± 0.8
8d	$-CH_2$-Ph	H	318 ± 110	0.30 ± 0.12	158 ± 42	6.4 ± 4.0	3.9 ± 0.6
8e	$-CH_2$-*c*-pentyl	H	177 ± 182	0.15 ± 0.02	48 ± 2	3.1 ± 0.2	3.0 ± 0.4
8f	4-Cl-Ph	H	71 ± 0	**0.046 ± 0.002**	27 ± 5	3.3 ± 0.2	1.8 ± 0.9
8g	3,4-diCl_2Ph	H	75 ± 49	**0.042 ± 0.008**	30 ± 2	2.7 ± 0.3	0.99 ± 0.53
8h	2-pyridinyl	H	316 ± 17	1.3 ± 0.4	46 ± 1	3.1 ± 0.2	3.8 ± 0.1
8i	H	Ph	≥500	1.1 ± 0.6	445 ± 78	19 ± 3	17 ± 0
8j	H	4-Cl-Ph	109 ± 79	4.0 ± 0.0	392 ± 18	30 ± 0	30 ± 4
14a	Ph		> 500	0.25 ± 0.09	36 ± 6	3.7 ± 0.5	2.9 ± 0.8
14b	4-Cl-Ph		> 500	**0.036 ± 0.003**	4.5 ± 0.6	1.7 ± 0.4	0.46 ± 0.06
15			> 500	> 500	> 500	> 500	> 500
6			316 ± 1.2	0.15 ± 0.01	195 ± 54	24 ± 3.0	

[a] IC_{50} is the 50% inhibitory concentration of the test compounds, which was measured as the concentration required to inhibit 1 μM [CH_3-^{3}H]dThd phosphorylation by 50%. The K_m values of TK-1, TK-2, HSV-1 TK, VZV TK, and Dm dNK for the natural substrate dThd were 2.3, 1.1, 1.44, 3.4, and 3.5 μM, respectively.

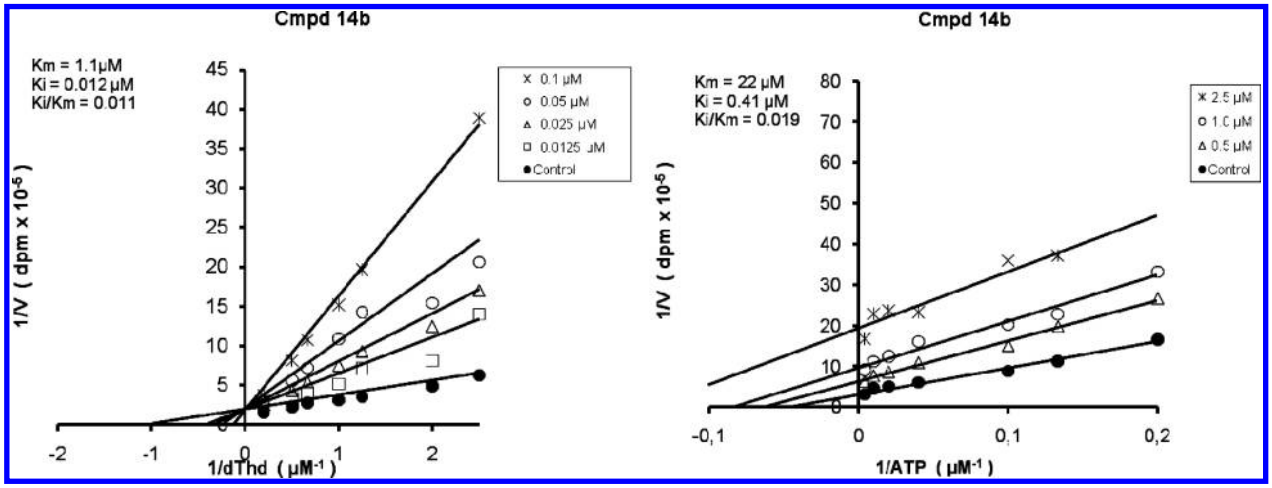

Figure 1. Kinetics of **14b** against purified recombinant mitochondrial TK-2.

lower than 1 (0.011), pointing to an affinity for the enzyme that largely exceeds the affinity of the natural substrate. Second, the K_i values of this inhibitor were also determined in the presence of a fixed saturating concentration of dThd and variable concentrations of the cosubstrate ATP. Compound **14b** showed a K_i value that was higher (0.41 μM) than that observed in the presence of dThd as the variable substrate. However, the K_i/K_m ratio was again much lower than 1 (0.019). Interestingly, under these conditions, **14b** behaved kinetically differently and displayed an uncompetitive mechanism of enzyme inhibition, as revealed by the (virtually) parallel kinetic lines in the Lineweaver−Burk plots.

These features point toward a specific binding of the inhibitor to an enzyme−ATP complex. Compound **15** was synthesized to assess the compatibility of combining the thiourea moiety of **6** with a 5′-*O*-trityl group. Combination of the 3′-modification and the 5′-*O*-trityl substituent led, as expected, to an analogue that was completely devoid of affinity for TK-2.

Molecular Modeling and Structure−Activity Relationship. To gain insight into the mode of binding of this new class of

inhibitors, docking experiments were undertaken using the previously reported homology-based model of TK-2 as the target.[11] This model is largely, but not exclusively, based on many similarities with the well-characterized structure of Dm-dNK although two relatively major uncertainties remain: (i) the conformation of the C-terminal low-homology His-rich loop that stabilizes the adenine ring of ATP in its binding site (as no C-terminally truncated dNK has been cocrystallized with ATP bound in the cofactor-binding site), and (ii) the precise side chain conformation of residues making up the loop that closes the entrance to the active site and stabilizes ATP (and, in our case, also inhibitor) binding. This "lid loop" appears as a disordered region in many dNK crystal structures apparently due to its high mobility, and side chain orientation varies depending on the nature of the molecules binding in the long active-site cleft and on the presence of an additional negative charge (e.g., sulfate ions) on the enzyme surface.

Through extrapolation from available data for Dm-dNK (in complex with drugs, substrates and "feedback-inhibiting" deoxyribonucleoside triphosphates) we can safely assume for human TK-2 that:

(1) In the presence of bound ATP-Mg^{2+}, the lid region (R[196]CREEEK[202]) must be found in the closed conformation, with Glu200 establishing a strong ionic interaction with the guanidinium of Arg87 and also a hydrogen bond with the carboxamide nitrogen of Asn93, whereas the carboxylate of Glu201 interacts strongly with the guanidinium groups of Arg196 and Arg198, which in turn are crucial for the anchoring of the α and β phosphate groups, respectively, of ATP.

(2) The 3′-OH of the thymidine substrate can be held in place with the aid of two direct hydrogen bonds, one with the carboxylate of Glu201 and another one with the phenol of Tyr99. This latter group is further anchored due to the intervention of a water molecule that bridges additional hydrogen bonds with the hydroxyl of Tyr208 and the O2 atom of the thymine base. The presence of a positionally equivalent water molecule and a similar extended hydrogen bonding network is a constant feature in available crystallographic structures of Dm-dNK.[25]

(3) The presence of Mg^{2+} bound to the ATP phosphates promotes a small displacement of the side chains of Glu81 and Glu133 with respect to their positions in the absence of this metal ion so that two carboxylate oxygens from these residues become part of the coordination sphere of the cation, which is also fixed in position by the hydroxyl of Thr64 (also hydrogen-bonded to Glu133) and two phosphate groups from ATP.

(4) As previously proposed for **6** and related thiourea-derived inhibitors,[11] the thymine ring of β-thymidine-containing compounds can stack on the phenyl ring of Phe143, whereas O4 and N3 atoms are held in place by virtue of two highly directional hydrogen bonds with the carboxamide group of Gln110 (equivalent to Gln81 in Dm-dNK). On the other hand, a free O5′-hydroxyl of a nucleosidic ligand can be hydrogen-bonded by the guanidinium nitrogen of Arg134 and the carboxylate of Glu81, whose equivalent residues in Dm-dNK have been shown to be crucial for the phosphoryl transfer reaction.[26] Thus, on the basis of the results from multiple sequence alignments (Supporting Information) and the homology-built model presented herein, Glu81 in TK-2 most likely acts as the base that deprotonates the 5′-OH of thymidine, whereas Arg134 plays a crucial role in the stabilization of the transition state during the phosphoryl transfer reaction.

An interesting observation in Dm-dNK is that when a triphosphate-Mg^{2+} cluster is present in the P-loop region of the ATP-binding site (e.g., from the dTTP feedback inhibitor, as in PDB entry 2VP0), the carboxylate of Glu52 (positionally and functionally equivalent to Glu81 in TK-2), which hydrogen bonds to the 5′-OH of the substrate and also to the guanidinium of Arg105 (Arg134 in TK-2) in the complexes of the enzyme with deoxynucleosides (e.g., 1J90), is slightly displaced and exchanges partners so as to enter the coordination sphere of the Mg^{2+} ion. When this happens, the guanidinium of Arg105 turns around and interacts with the phosphate group that will be transferred to the 5′-OH of the substrate as well as with the carboxylate of Glu26 (a residue that is also used to establish a strong hydrogen bond with the hydroxyl of the highly conserved Ser106 present in the ERS motif). In both conformational states, however, the buried position of the guanidinium of Arg105, which makes up the "floor" of the triphosphate binding site under the P-loop "ceiling", is guaranteed by a direct interaction with the carbonyl oxygen of Gly27.

Taking all TK-2's conformational features into account, our best docking solution for **8f**, supported and refined by subsequent MD simulation in water, suggests that the thymidine moiety of this inhibitor fills the same volume that is usually occupied by the substrate thus giving rise to the interactions described above for deoxythymidine (Figure 2). In this location, the C2′-endo puckering of the sugar ring places the triazole ring at the 3′ position with its nitrogens facing Glu200 (the middle Glu in the EEE lid region, and positionally and functionally equivalent to Glu171 in Dm-dNK) and the attached phenyl ring forces the side-chain of Tyr99 (the equivalent to Tyr70 in Dm-dNK), to change its orientation through a flipping motion and also displaces the bound water molecule described above. Interestingly, interaction with the carboxylate of Glu200 happens to be mediated by a bridging water molecule that is also bonded to Arg198. As these two residues are part of the lid loop, this arrangement can account for the fact that the loop is closed over the active site and therefore the ATP molecule can get trapped. At this point it is worth noting that a 180° rotation of the triazole ring relative to the sugar would lead to steric clash of the attached phenyl ring with the lid loop and also that this model does not favor substitution at position 5 of the triazole ring, in good agreement with the much lower inhibitory activity measured for the 1,5-substituted derivatives **8i** and **8j**. On the contrary, this binding orientation is fully compatible with the modulation of the inhibitory activity upon introduction of substituents at position 4. Incidentally, in the few protein-bound ligands containing a 1,2,3-triazole ring available from the Protein Data Bank (entries 1VM1, 1ZP8, and 1ZPA) this moiety is consistently involved in an intra- or intermolecular hydrogen bond with a water molecule.

It is important to highlight that the model provides an explanation to the 10-fold improvement in activity that is achieved upon incorporation of the phenyl ring to the unsubstituted triazole derivative **8a**. This phenyl ring in **8f**

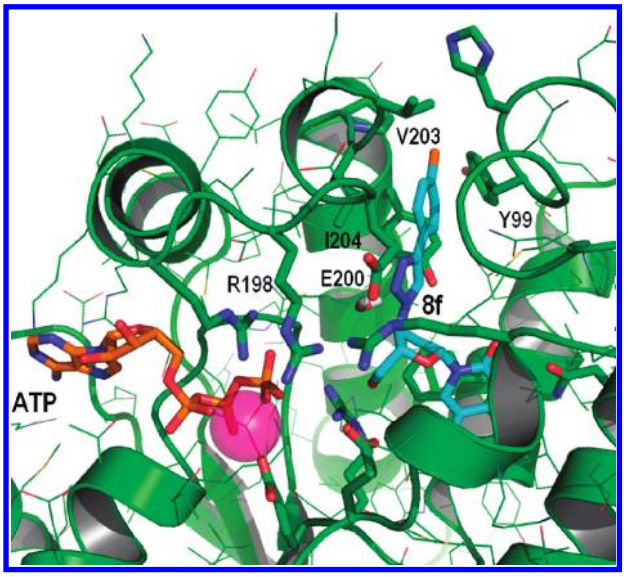

Figure 2. Proposed binding mode for inhibitor **8f** (C atoms in cyan), in the active site of human TK-2 (green ribbon). ATP is shown as sticks, with C atoms colored in orange, and Mg^{2+} is displayed as a semitransparent sphere colored in magenta. Some of the protein side chains relevant to the discussion are labeled and shown as sticks. Note the "close" conformation of the lid loop that normally covers the substrate-binding cleft during catalysis and the water molecule that bridges the interaction between the triazole of the inhibitor and the carboxylate of Glu200.

is proposed to make van der Waals interactions with Val203 and Ile204 within the VIPLEY sequence that immediately follows the lid loop so that these hydrophobic contacts can contribute to stabilization of the closed form of the enzyme. We are also aware that these proposed interactions are more favorable in TK-2 than those possible with the Cys and Val of CVPLKY in Dm-dNK. Taken together, sequence differences at these positions can account for the better inhibition of human TK-2 relative to Dm-dNK by the title compounds. On the other hand, comparison with **8f** reveals the importance for activity of the chlorine atom at the para position (but not of the addition of a second chlorine in meta, as in compound **8g**) and the deleterious effect of replacing the phenyl with a 2-pyridinyl substituent, as in compound **8h**. It is also interesting to note that **14a** and **14b**, both containing a BVDU moiety in place of the thymine, are only marginally more potent than **8c** and **8f**, respectively, an observation that is in line with the facts that (i) the K_m value of BVDU when used as a substrate for Dm-DNK is only ~4-fold lower than that of AZT,[24] (ii) the nucleobase-binding site in Dm-DNK and human TK2 are highly comparable, and (iii) AZT and BVDU binding to Dm-DNK show similar characteristics, as inferred from comparison of PDB structures 2JJ8 and 2VQS. Finally, our finding that a 5′-*O*-trityl substituent renders the inhibitors in the present series inactive is also consistent with the proposed binding mode insofar as the 5′-hydroxyl is used, as described above and reported previously for thiourea-derived inhibitors,[11] to anchor the inhibitor in the substrate binding site through hydrogen bonding interactions with the catalytically important Arg134 and Glu81.

To reveal whether the TK-2 inhibitors are able to be taken up by the cells, the most active compound **14b** was chosen for further studies. Because of the lack of TK-2 gene-transduced tumor cells, human osteosarcoma cells (OST TK^-) were used that were transfected with the *Drosophila melanogaster* multifunctional deoxynucleoside kinase gene (*OST* TK^-/*Dm* dNK^+). Alike TK-2, the Dm dNK enzyme is sensitive to the inhibitory activity of compound **14b** at an IC_{50} of 0.46 μM (Table 3). The cytostatic agents (*E*)-5-(2-bromovinyl)-2′-deoxyuridine (BVDU) and 5-fluoro-2′-deoxyuridine (5FdUrd) were exposed to these cell cultures in the presence or absence of **14b** (used at subtoxic concentrations (10 μM and 4 μM)) (Table 4). Whereas BVDU and 5FdUrd were cytostatic at an IC_{50} of 0.76 and 0.066 μM, respectively, their antiproliferative effect was significantly (4-fold) decreased in the presence of **14b** at 10 μM (IC_{50}: 2.95 and 0.263 μM, respectively) and at 4 μM (IC_{50}: 1.64 and 0.110 μM, respectively). Thus, the conversion of BVDU and 5FdUrd to their toxic metabolite(s) by Dm dNK could be dose-dependently blocked by 80% in the presence of the TK-2 (Dm dNK) inhibitor under the experimental conditions. These data revealed that the TK-2 inhibitors such as **14b** can enter the intact tumor cells and be inhibitory to the nucleoside kinase present in the cytosol. It would now be imperative to investigate whether these compounds are also taken up by mitochondria after their penetration into the intact cells, enabling targeting TK-2 in the mitochondrial environment.

Table 4. Cytostatic Activity of BVDU and 5FdUrd against Dm dNK-Expressing OST TK^-/Dm dNK^+ Cells in the Absence or Presence of Compound **14b**

	IC_{50}[a] (μM)		
		compd **14b**	
compd	as such	10 μM	4 μM
BVDU	0.76 ± 0.001	2.95 ± 0.96	1.64 ± 0.07
5FdUrd	0.066 ± 0.003	0.263 ± 0.104	0.110 ± 0.035

[a] 50% Inhibitory concentration or compound concentration required to inhibit OST TK^-/dNK^+ cell proliferation by 50%. Data are the mean ± SD of two independent experiments. The IC_{50} of compound **14b** as such is 23 ± 15 μM.

Conclusions

Cycloaddition of organic azides and alkynes is the most direct route to 1,2,3-triazoles. In this study, we used two different catalysts to achieve this reaction: the Cu(I) catalyst, which provided the 1,4-disubstituted 1,2,3-triazole regioisomers, and the [Cp*RuClP$(Ph_3)_2$] catalyst, which has recently been described for regioselective synthesis of 1,5-disubstituted 1,2,3-triazole systems.

By replacing the thiourea linker of an earlier identified TK-2 inhibitor **6** by a 1,4-substituted triazole ring, we successfully generated a new generation of very potent TK-2 inhibitors. Combining such a favorable sugar modification with a bromovinyl substituent at position 5 of the pyrimidine moiety further enhanced the selectivity vis-à-vis TK-1.

The direct interaction between the triazole moiety and the γ-phosphate group of ATP that was envisioned at the outset of this project was not supported by our docking and simulation studies. Instead, our results strongly suggest that the triazole appears to displace, through a flipping motion, the side chain of a tyrosine residue (Tyr99) that is involved in anchoring the 3′-OH of the substrate in the thymidine binding pocket. Relatively small readjustments allow the triazole N2 atom to hydrogen bond the carboxylate of Glu200 from the lid loop through the intervention of a bridging water molecule that is also hydrogen-bonded to the side-chain of Arg198. This orientation allows the phenyl ring attached at position 4 of the triazole to occupy a hydrophobic cavity and increase the binding affinity. Thus, we propose that the best inhibitors in

this series stabilize, through a well-defined set of interactions, a closed conformation of the enzyme that traps an ATP molecule in the cofactor binding site. This binding mode provides a rationale to the biochemical evidence and an explanation to the structure−activity relationship in atomic detail.

Experimental Section

Synthesis. General. All reagents were from standard commercial sources and of analytic grade. Precoated Merck silica gel F254 plates were used for TLC, spots were examined under ultraviolet light at 254 nm and further visualized by sulfuric acid-anisaldehyde spray. Column chromatography was performed on silica gel (63−200 μm, 60 Å, Biosolve, Valkenswaard, The Netherlands). NMR spectra were determined using a Varian Mercury 300 MHz spectrometer. Chemical shifts are given in ppm (δ) relative to the residual solvent signals, which in the case of DMSO-d_6 were 2.54 ppm for ^{1}H and 40.5 ppm for ^{13}C. Structural assignment was confirmed with COSY and DEPT. All signals assigned to hydroxyl groups were exchangeable with D_2O. Exact mass measurements were performed on a Waters LCT Premier XETM Time of flight (TOF) mass spectrometer equipped with a standard electrospray ionization (ESI) and modular LockSpray TM interface. Samples were infused in a CH_3CN/water (1:1) mixture at 10 μL/min. Elemental analyses were performed with a Heraeus CHN-O-Rapid instrument and are within 0.4% of theoretical values unless otherwise specified.

3′-(1,2,3-Triazol-1-yl)-3′-deoxy-β-D-thymidine (8a). To a solution of trimethylsilylacetylene (85 μL, 0.59 mmol) in 3 mL of ^{t}BuOH/H_2O 1:1 (v:v) was added sodium ascorbate (18 mg, 0.089 mmol) and $CuSO_4 \cdot 5H_2O$ (11 mg, 0.044 mmol). The mixture was stirred for 15 min. **7** (80 mg, 0.30 mmol) was added, and the resulting mixture was stirred at 45 °C for 24 h. The reaction mixture was washed with ethyl acetate (3 × 5 mL), and the combined organic phases were washed with water, dried over anhydrous Na_2SO_4, and evaporated to dryness. Without further purification, 1.0 M TBAF in THF was added (1.2 mL) and the mixture was stirred at room temperature. After 16 h, TLC analysis revealed almost complete disappearance of all starting material. The solvent was evaporated and the mixture purified by column chromatography (EtOAc/MeOH, 100:0 → 95:5) yielding **8a** as a white powder (35 mg, 40%). ^{1}H NMR (300 MHz, DMSO-d_6): δ 1.79 (3H, d, J = 0.9 Hz, 5-CH_3), 2.63−2.72 (2H, m, H-2′a and H-2′b), 3.58−3.71 (2H, m, H-5′a and H-5′b), 4.17−4.21 (1H, m, H-4′), 5.21−5.32 (1H, m, 5′-OH), 5.37−5.39 (1H, m, H-3′), 6.41 (1H, app t, J = 6.3 Hz, H-1′), 7.78 (1H, d, J = 0.9 Hz, H-4″), 7.81 (1H, d, J = 1.2 Hz, H-6), 8.30 (1H, d, J = 0.9 Hz, H-5″), 11.33 (1H, s, 3-NH). ^{13}C NMR (75 MHz, DMSO-d_6): δ 12.27 (5-CH_3), 37.22 (C-2′), 58.97 (C′-5), 60.72 (C-3′), 83.89 (C-1′), 84.52 (C-4′), 109.63 (C-5), 124.49 (C-5″), 133.57 (C-4″), 136.26 (C-6), 150.45 (C-2), 163.74 (C-4). HRMS (ESI-MS) for $C_{12}H_{16}N_5O_4$ $[M + H]^+$ found, 350.1820; calcd, 350.1823. Anal. ($C_{12}H_{15}N_5O_4$) C, H, N.

General Procedure for the Synthesis of 4″-Substituted 3′-Deoxy-3′-(1,2,3-Triazol-1-yl)-β-D-thymidine Derivatives 8b−8h. Compound **7** (1 mmol, 1 equiv), sodium ascorbate (0.05 equiv), and $CuSO_4 \cdot 5H_2O$ (0.04 equiv) were suspended in 10 mL of ^{t}BuOH/H_2O (1:1). The appropriate alkyne (2 equiv) was added after 15 min, and the mixture was stirred at room temperature for 24 h. The reaction mixture was washed with CH_2Cl_2, and the combined organic phases were washed with water, dried over anhydrous $MgSO_4$, and evaporated to dryness. The crude product was purified by column chromatography, affording the triazole in moderate yield.

3′-(4-Butyl-1,2,3-triazol-1-yl)-3′-deoxy-β-D-thymidine (8b). The reaction of **7** (66 mg, 0.24 mmol) with 1-hexyne (60 μL, 0.49 mmol) gave compound **8b** (47 mg, 55%) as a white powder. ^{1}H NMR (300 MHz, DMSO-d_6): δ 0.90 (3H, t, J = 7.2 Hz, butyl), 1.24−1.40 (2H, m, butyl), 1.54−1.64 (2H, m, butyl), 1.79 (3H, d, J = 0.9 Hz, 5-CH_3), 2.58−2.77 (4H, m, H-2′a, H-2′b and butyl), 3.53−3.72 (2H, m, H-5′a and H-5′b), 4.14−4.18 (1H, m, H-4′), 5.26−5.31 (2H, m, H-3′ and 5′−OH), 6.40 (1H, app t, J = 6.6 Hz, H-1′), 7.81 (1H, d, J = 1.2 Hz, 6-H), 8.04 (1H, s, H-5″), 11.33 (1H, s, 3-NH). ^{13}C NMR (75 MHz, DMSO-d_6): δ 12.26 (5-CH_3), 13.71, 22.71, 24.70, and 31.03 (butyl), 37.12 (C-2′), 58.95 (C-5′), 60.76 (C-3′), 83.88 (C-1′), 84.51 (C-4′), 109.63 (C-5), 121.39 (C-5″), 136.27 (C-6), 147.22 (C-4″), 150.46 (C-2), 163.76 (C-4). HRMS (ESI-MS) for $C_{16}H_{24}N_5O_4$ $[M + H]^+$ found, 350.1820; calcd, 350.1823. Anal. ($C_{16}H_{23}N_5O_4$) C, H, N.

3′-Deoxy-3′-(4-phenyl-1,2,3-triazol-1-yl)-β-D-thymidine (8c). The reaction of **7** (50 mg, 0.19 mmol) with phenylacetylene (41 μL, 0.37 mmol) afforded compound **8c** in 72% yield (49 mg). ^{1}H NMR (300 MHz, DMSO-d_6): δ 1.82 (3H, d, J = 0.9 Hz, 5-CH_3), 2.65−2.86 (2H, m, H-2′a and H-2′b), 3.61−3.77 (2H, m, H-5′a and H-5′b), 4.27−4.31 (1H, m, H-4′), 5.31 (1H, app br s, 5′-OH), 5.38−5.45 (1H, m, H-3′), 6.46 (1H, app t, J = 6.3 Hz, H-1′), 7.33−7.38 (1H, m, Ph), 7.44−7.49 (2H, m, Ph), 7.85−7.88 (3H, m, Ph and H-6), 8.78 (1H, s, H-5″), 11.36 (1H, s, 3-NH). ^{13}C NMR (75 MHz, DMSO-d_6): δ 12.27 (5-CH_3), 37.15 (C-2′), 59.37 (C-5′), 60.76 (C-3′), 83.90 (C-1′), 84.43 (C-4′), 109.65 (C-5), 121.01 (C-5″), 125.17, 128.00, 128.95, and 130.58 (Ph), 136.26 (C-6), 146.57 (C-4″), 150.46 (C-2), 163.75 (C-4). HRMS (ESI-MS) for $C_{18}H_{20}N_5O_4$ $[M + H]^+$ found, 370.1517; calcd, 370.1510. Anal. ($C_{18}H_{19}N_5O_4$) C, H, N.

3′-(4-Benzyl-1,2,3-triazol-1-yl)-3′-deoxy-β-D-thymidine (8d). The reaction of **7** (50 mg, 0.19 mmol) with 3-phenyl-1-propyne (58 μL, 0.47 mmol) gave compound **8d** (42 mg, 59%) as a white powder. ^{1}H NMR (300 MHz, DMSO-d_6): δ 1.80 (3H, d, J = 1.2 Hz, 5-CH_3), 2.56−2.75 (2H, m, H-2′a and H-2′b), 3.53−3.64 (2H, m, H-5′a and H-5′b), 4.00 (2H, s, Bn), 4.16−4.20 (1H, m, H-4′), 5.24−5.34 (2H, m, 5′-OH and H-3′), 6.40 (1H, app t, J = 6.6 Hz, H-1′), 7.18−7.33 (5H, m, Bn), 7.80 (1H, d, J = 1.2 Hz, H-6), 8.03 (1H, s, H-5″), 11.33 (1H, s, 3-NH). ^{13}C NMR (75 MHz, DMSO-d_6): δ 12.24 (5-CH_3), 31.28 (Bn), 37.08 (C-2′), 59.05 (C-5′), 60.75 (C-3′), 83.83 (C-1′), 84.43 (C-4′), 109.60 (C-5), 122.15 (C-5″), 126.20, 128.44, and 128.56 (Bn), 136.23 (C-6), 139.41 (Bn), 146.34 (C-4″), 150.43 (C-2), 163.72 (C-4). HRMS (ESI-MS) for $C_{19}H_{22}N_5O_4$ $[M + H]^+$ found, 384.1672; calcd, 384.1666. Anal. ($C_{19}H_{21}N_5O_4$) C, H, N.

3′-(4-Cyclopentylmethyl-1,2,3-triazol-1-yl)-3′-deoxy-β-D-thymidine (8e). The reaction of **7** (89 mg, 0.33 mmol) with 3-cyclopentyl-1-propyne (88 μL, 0.66 mmol) yielded compound **8e** (86 mg, 69%) as a white powder. ^{1}H NMR (300 MHz, DMSO-d_6): δ 1.16−1.23 (2H, m, cyclopentyl), 1.46−1.59 (4H, m, cyclopentyl), 1.76−1.76 (2H, m, cyclopentyl), 1.81 (3H, d, J = 1.2 Hz, 5-CH_3), 2.06−2.16 (1H, m, cyclopentyl), 2.44−2.63 (4H, m, H-2′a, H-2′b and CH_2), 3.60−3.63 (2H, m, H-5′a and H-5′b), 4.14−4.21 (1H, m, H-4′), 5.22−5.35 (2H, m, H-3′ and 5′-OH), 6.40 (1H, app t, J = 6.6 Hz, H-1′), 7.81 (1H, d, J = 1.2 Hz, 6-H), 8.04 (1H, s, H-5″), 11.33 (1H, s, 3-NH). ^{13}C NMR (75 MHz, DMSO-d_6): δ 12.24 (5-CH_3), 24.61 (cyclopentlyl), 31.07 (CH_2), 31.91 (cyclopentyl), 37.06 (C-2′), 58.88 (C-5′), 60.90 (C-3′), 83.83 (C-1′), 84.47 (C-4′), 109.60 (C-5), 121.63 (C-5″), 136.25 (C-6), 146.71 (C-4″), 150.43 (C-2), 163.72 (C-4). HRMS (ESI-MS) for $C_{18}H_{26}N_5O_4$ $[M + H]^+$ found, 376.1975; calcd, 376.1979. Anal. ($C_{18}H_{25}N_5O_4$) C, H, N.

3′-(4-Chlorophenyl-1,2,3-triazol-1-yl)-3′-deoxy-β-D-thymidine (8f). The reaction of **7** (70 mg, 0.26 mmol) with 1-chloro-4-ethynylbenzene (72 mg, 0.52 mmol) yielded compound **8f** (15 mg, 14%) as a light-gray powder. ^{1}H NMR (300 MHz, DMSO-d_6): δ 1.82 (3H, d, J = 1.2 Hz, 5-CH_3), 2.63−2.85 (2H, m, H-2′a and H-2′b), 3.60−3.74 (2H, m, H-5′a and H-5′b), 4.22−4.32 (1H, m, H-4′), 5.28−5.34 (1H, m, 5′-OH), 5.36−5.44 (1H, m, H-3′), 6.42 (1H, app t, J = 6.6 Hz, H-1′), 7.52−7.56 (2H, m, Ph), 7.83 (1H, d, J = 1.2 Hz, 6-H), 7.86−7.91 (2H, m, Ph), 8.83 (1H, s, H-5″), 11.33 (1H, s, 3-NH). ^{13}C NMR (75 MHz, DMSO-d_6): δ 12.26 (5-CH_3), 37.13 (C-2′), 59.47 (C-5′), 60.76 (C-3′), 83.89 (C-1′), 84.41 (C-4′), 109.71 (C-5), 121.38 (C-5″), 126.86, 128.81, 129.03, 129.33, 129.49, and 132.42 (4-chlorophenyl), 136.25 (C-6), 145.49 (C-4″), 150.44 (C-2), 163.73 (C-4). HRMS (ESI-MS) for $C_{18}H_{19}ClN_5O_4$ $[M + H]^+$ found, 404.1129; calcd, 404.1120. Anal. ($C_{18}H_{18}ClN_5O_4$) C, H, N.

3′-Deoxy-3′-(4-(3,4-dichlorophenyl)-1,2,3-triazol-1-yl)-β-D-thymidine (8g). The reaction of **7** (67 mg, 0.25 mmol) with 3,4-dichlorophenylacetylene (88 mg, 0.50 mmol) afforded compound **8g** (25 mg, 25%) as a white powder. ^{1}H NMR (300 MHz, DMSO-d_6): δ 1.82 (3H, d, J = 0.9 Hz, 5-CH_3), 2.71−2.80 (2H, m, H-2′a and H-2′b), 3.64−3.77 (2H, m, H-5′a and H-5′b), 4.25−4.29 (1H, m, H-4′), 5.32 (1H, t, J = 5.1 Hz, 5′-OH), 5.37−5.43 (1H, m, H-3′), 6.42 (1H, app t, J = 6.9 Hz, H-1′), 7.72 (1H, d, J = 8.7 Hz, 3,4-dichlorophenyl), 7.82−7.87 (2H, m, 3,4-dichlorophenyl), 8.08 (1H, d, J = 1.8 Hz, 6-H), 8.93 (1H, s, H-5″). ^{13}C NMR (75 MHz, DMSO-d_6): δ 12.26 (5-CH_3), 37.06 (C-2′), 59.60 (C-5′), 60.76 (C-3′), 83.89 (C-1′), 84.43 (C-4′), 109.66 (C-5), 122.08 (C-5″), 125.18, 126.78, 130.26, 131.27, 131.32, and 131.77 (3,4-dichlorophenyl), 136.23 (C-6), 144.37 (C-4″), 150.44 (C-2), 163.73 (C-4). HRMS (ESI-MS) for $C_{18}H_{18}Cl_2N_5O_4$ $[M + H]^+$ found, 438.0745; calcd, 438.0730. Anal. ($C_{18}H_{17}Cl_2N_5O_4$) C, H, N.

3′-Deoxy-3′-(4-pyridin-2-yl-1,2,3-triazol-1-yl)-β-D-thymidine (8h). The reaction of **7** (74 mg, 0.28 mmol) with 2-ethynylpyridine (57 mg, 0.55 mmol) gave compound **8h** (22 mg, 21%) as a light-gray powder. ^{1}H NMR (300 MHz, DMSO-d_6): δ 1.82 (3H, d, J = 1.2 Hz, 5-CH_3), 2.64−2.73 (1H, m, H-2′a), 2.79−2.88 (1H, m, H-2′b), 3.64−3.80 (2H, m, H-5′a and H-5′b), 4.27−4.32 (1H, m, H-4′), 5.34−5.25 (1H, m, 5′-OH), 5.43−5.52 (1H, m, H-3′), 6.46 (1H, app t, J = 6.9 Hz, H-1′), 7.34−7.39 (1H, m, pyridin-2-yl), 7.84 (1H, d, J = 1.2 Hz, 6-H), 7.88−7.94 (1H, m, pyridin-2-yl), 8.04−8.07 (1H, m, pyridin-2-yl), 8.60−8.63 (1H, m, pyridin-2-yl), 8.83 (1H, s, H-5″), 11.31 (1H, s, 3-NH). ^{13}C NMR (75 MHz, DMSO-d_6): δ 12.26 (5-CH_3), 37.14 (C-2′), 59.46 (C-5′), 60.73 (C-3′), 83.88 (C-1′), 84.40 (C-4′), 109.65 (C-5), 119.47 (pyridin-2-yl), 122.94 (C-5″), 123.11 (pyridin-2-yl), 136.30 (C-6), 137.27 (pyridin-2-yl), 147.46 (C-4″), 149.72 (pyridin-2-yl), 150.45 (C-2), 163.74 (C-4). HRMS (ESI-MS) for $C_{17}H_{19}N_6O_4$ $[M + H]^+$ found, 371.1461; calcd, 371.1462. Anal. ($C_{17}H_{18}N_6O_4$) C, H, N.

General Procedure for the Synthesis of 5″-Substituted 3′-Deoxy-3′-(1,2,3-triazol-1-yl)-β-D-thymidine Derivatives 8i−8j. The appropriate alkyne (2 equiv) and Cp*RuCl(PPh_3)$_2$ (0.02 equiv) were added to a solution of **7** (1 mmol, 1 equiv) in 5 mL of THF. The mixture was stirred at 65 °C, and after several hours the reaction was stopped. The solvent was removed and the residue redissolved in CH_2Cl_2, washed with water (3 × 10 mL), dried over $MgSO_4$, and evaporated in vacuum. Purification with column chromatography afforded the 5″-substituted triazole.

3′-Deoxy-3′-(5-phenyl-1,2,3-triazol-1-yl)-β-D-thymidine (8i). The reaction of **7** (66 mg, 0.25 mmol) with phenylacetylene (50 μL, 0.50 mmol) afforded compound **8i** (26 mg, 29%) as a white powder. ^{1}H NMR (300 MHz, DMSO-d_6): δ 1.77 (3H, d, J = 1.2 Hz, 5-CH_3), 2.56−2.63 (2H, m, H-2′a and H-2′b), 3.47−3.53 (1H, m, H-5′a), 3.54−3.64 (1H, m, H-5′b), 4.39 (1H, app dt, J = 3.6 Hz; H-4′), 5.14−5.19 (1H, m, H-3), 5.22−5.27 (1H, m, 5′-OH), 6.56 (1H, app t, J = 6.3 Hz, H-1′), 7.53−7.63 (5H, m, Ph), 7.77 (1H, d, J = 1.2 Hz, 6-H), 7.92 (1H, s, H-4″), 11.35 (1H, s, 3-NH). ^{13}C NMR (75 MHz, DMSO-d_6): δ 12.45 (5-CH_3), 38.00 (C-2′), 58.57 (C-5′), 61.50 (C-3′), 84.97 (C-1′), 85.12 (C-4′), 110.03 (C-5), 126.49, 129.44, and 129.90 (Ph), 133.16 (C-5″), 136.45 (C-6), 138.22 (C-4″), 150.65 (C-2), 163.96 (C-4). HRMS (ESI-MS) for $C_{18}H_{20}N_5O_4$ $[M + H]^+$ found, 370.1512; calcd, 370.1510. Anal. ($C_{18}H_{19}N_5O_4$) C, H, N.

3′-(5-(4-Chlorophenyl)-1,2,3-triazol-1-yl)-3′-deoxy-β-D-thymidine (8j). The reaction of **7** (52 mg, 0.19 mmol) with 1-chloro-4-ethynylbenzene (55 mg, 0.40 mmol) yielded compound **8j** (19 mg, 20%) as a white solid. ^{1}H NMR (300 MHz, DMSO-d_6): δ 1.78 (3H, app s, 5-CH_3), 2.44−2.65 (2H, m, H-2′a and H-2′b), 3.46−3.52 (1H, m, H-5′a), 3.57−3.63 (1H, m, H-5′b), 4.37−4.41 (1H, m, H-4′), 5.11−5.14 (1H, m, H-3′), 5.19−5.25 (1H, m, 5′-OH), 6.54 (1H, app t, J = 6.6 Hz, H-1′), 7.56−7.66 (4H, m, Ph), 7.76 (1H, app s, H-6), 7.95 (1H, s, H-4″), 11.35 (1H, s, 3-NH). ^{13}C NMR (75 MHz, DMSO-d_6): δ 12.94 (CH_3), 38.41 (C-2′), 59.06 (C-5′), 62.03 (C-3′), 85.33 (C-1′), 85.51 (C-4′), 110.39 (C-5), 125.98, 129.86, and 131.83 (4-chlorophenyl), 133.84 (C-5″), 135.22 (C-4″), 136.80 (C-6), 137.53 (4-chlorophenyl), 151.13 (C-2), 164.34 (C-4). HRMS (ESI-MS) for $C_{18}H_{19}ClN_5O_4$ $[M + H]^+$ found, 404.1120; calcd, 404.1120. Anal. ($C_{18}H_{18}ClN_5O_4$) C, H, N.

5′-*O*-Triphenylmethyl-β-(*E*)-5-(2-bromovinyl)-2′-deoxyuridine (10). To a solution of (*E*)-5-(2-bromovinyl)-2′-deoxyuridine (**9**) (0.467 g, 1.40 mmol) in anhydrous pyridine (3 mL) was added DMAP (0.189 g, 1.54 mmol) and trityl chloride (0.460 g, 1.65 mmol). The mixture was heated to 65 °C and stirred overnight. The reaction mixture was then diluted with CH_2Cl_2 (3 mL), washed with saturated aqueous $NaHCO_3$ (3 × 10 mL), and dried over anhydrous $MgSO_4$. The solvent was removed under reduced pressure, and the resulting residue was purified by column chromatography (CH_2Cl_2/MeOH 94:6), affording **10** as a white foam (0.482 g, 65%). ^{1}H NMR (300 MHz, DMSO-d_6): δ 2.12−2.31 (2H, m, H-2′a and H-2′b), 3.13−3.24 (2H, m, H-5′a and H-5′b), 3.86−3.90 (1H, m, H-4′), 4.24−4.27 (1H, m, H-3′), 5.32 (1H, d, J = 4,7 Hz, 3′−OH), 6.16 (1H, app t, J = 6,7 Hz, H-1′), 6.45 (1H, d, J = 13,5 Hz, bromovinyl), 7.18 (1H, d, J = 13,5 Hz, bromovinyl), 7.22−7.38 (15H, m, Tr), 7.72 (1H, s, H-6) 11.60 (1H, br s, 3-NH). ^{13}C NMR (75 MHz, DMSO-d_6): δ 38.69 (C-2′), 64.00 (C-5′), 70.06 (C-3′), 84.36 (C-1′), 85.47 (C-4′), 86.24 (Tr), 106.97 (C-5), 109.95 (bromovinyl), 123.91, 127.16, 127.97, 128.56, and 128.26 (Tr), 129.68 (bromovinyl), 139.32 (C-6), 148.52 (Tr), 149.26 (C-2), 161.68 (C-4). HRMS (ESI-MS) for $C_{30}H_{28}BrN_2O_5$ $[M + H]^+$ found, 575.1118; calcd, 575.1176.

2,3′-Anhydro-5′-*O*-triphenylmethyl-β-(*E*)-5-(2-bromovinyl)-2′-deoxyuridine (11). To an ice-cooled solution of **10** (0.482 g, 0.84 mmol) in pyridine (3 mL) was added methanesulfonyl chloride (0.20 mL, 2.51 mmol). The reaction mixture was stirred for 2 h, quenched with $NaHCO_3$, and extracted with ethyl acetate (3 × 10 mL). The combined organic layers were dried over $MgSO_4$ and evaporated to dryness. The residue was redissolved in 10 mL of ethano,l and dry triethylamine (0.68 mL, 4.88 mmol) was added. The mixture was heated, under reflux, for 18 h. The reaction was cooled, extracted with CH_2Cl_2 (3 × 10 mL), and the combined organic layers were dried over $MgSO_4$ and evaporated to dryness. The resulting residue was purified by column chromatography (CH_2Cl_2/MeOH 96:4), yielding **11** as a white foam (351 mg, 75%). ^{1}H NMR (300 MHz, DMSO-d_6): δ 2.43−2.67 (2H, m, H-2′a and H-2′b), 3.11−3.13 (2H, m, H-5′a and H-5′b), 4.43−4.49 (1H, m, H-4′), 5.38 (1H, app s, H-3′), 5.92 (1H, app d, J = 3.5 Hz, H-1′), 6.86 (1H, d, J = 13.5 Hz, bromovinyl), 7.20−7.41 (15H, m, Tr), 7.54 (1H, d, J = 13.5 Hz, bromovinyl), 7.96 (1H, s, H-6). ^{13}C NMR (75 MHz, DMSO-d_6): δ 32.73 (C-2′), 62.32 (C-5′), 77.55 (C-3′), 83.57 (C-1′), 86.39 (Tr), 87.57 (C-4′), 109.31 (C-5), 115.17 (bromovinyl), 127.06, 127.92, and 128.16 (Tr), 130.17 (bromovinyl), 139.62 (C-6), 143.22 (Tr), 152.29 (C-2), 168.07 (C-4). HRMS (ESI-MS) for $C_{30}H_{26}BrN_2O$ $[M + H]^+$ found, 557.1061; calcd, 557.1070.

3′-Azido-3′-deoxy-5′-*O*-triphenylmethyl-β-(*E*)-5-(2-bromovinyl)-2′-deoxyuridine (12). *p*-Nitrophenylalcohol (114 mg, 0.82 mmol) first and then NaN_3 (267 mg, 4.12 mmol) were added to a suspension of anhydronucleoside **11** (229 mg, 0.41 mmol) in dry DMF (5 mL) under N_2. The solution was stirred for 7 h at 110 °C. The reaction was quenched with 5 mL of water and extracted with CH_2Cl_2 (3 × 5 mL). The combined organic layers were dried over $MgSO_4$ and evaporated to dryness. The resulting residue was purified by column chromatography (CH_2Cl_2/MeOH 96:4), affording **12** as a yellow oil (195 mg, 79%). ^{1}H NMR (300 MHz, DMSO-d_6): δ 2.35−2.58 (2H, m, H-2′a and H-2′b), 3.25−3.40 (2H, m, H-5′a and H-5′b), 3.85−3.92 (1H, m, H-4′), 4.58 (1H, dt, J = 7.5 Hz, H-3′), 6.15 (1H, dd, J = 4.5 Hz, J = 7.2 Hz, H-1′), 6.64 (1H, d, J = 13.5 Hz, bromovinyl), 7.23−7.44 (16H, m, bromovinyl and Tr), 7.79 (1H, s, H-6). ^{13}C NMR (75 MHz, DMSO-d_6): δ 35.90 (C-2′), 59.16 (C-5′), 62.81 (C-3′), 82.11 (C-1′), 83.79 (C-4′), 86.37 (Tr), 110.12 (C-5), 115.79 (bromovinyl), 126.19, 127.05, 127.20, 127.86, 127.99, and 128.22 (Tr), 129.71 (bromovinyl), 139.59 (C-6), 143.38 (Tr), 149.23 (C-2), 161.63 (C-4). HRMS (ESI-MS) for $C_{30}H_{27}BrN_5O_4$ $[M + H]^+$ found, 600.1274; calcd, 600.1241.

3′-Azido-3′-deoxy-β-(*E*)-5-(2-bromovinyl)-2′-deoxyuridine (13). Compound **12** (260 mg, 0.43 mmol) was dissolved in a mixture of $ZnBr_2$ (1.59 g, 7.05 mmol) in CH_2Cl_2/^{i}PrOH (7 mL, 85:15) and stirred overnight at room temperature. The reaction was quenched with water and extracted with CH_2Cl_2 (3 × 10 mL). The combined organic layers were dried over $MgSO_4$ and evaporated to dryness. The resulting residue was purified by column chromatography (CH_2Cl_2/MeOH 98:2), affording **13** (139 mg, 90%) as a yellow−brown oil. ^{1}H NMR (300 MHz, DMSO-d_6): δ 2.31−2.44 (2H, m, H-2′a and H-2′b), 3.60−3.71 (2H, m, H-5′a and H-5′b), 3.80−3.86 (1H, m, H-4′), 4.38−4.44 (1H, m, H-3′), 5.30 (1H, app s, 5′−OH), 6.05−6.09 (1H, m, H-1′), 6.84 (1H, d, J = 13.8 Hz, bromovinyl), 7.25 (1H, d, J = 13.5 Hz, bromovinyl), 8.04 (1H, s, H-6). ^{13}C NMR (75 MHz, DMSO-d_6): δ 36.67 (C-2′), 54.92 (C-5′), 60.36 (C-3′), 84.12 (C-1′), 84.37 (C-4′), 106.60 (C-5), 109.71 (bromovinyl), 129.83 (bromovinyl), 139.38 (C-6), 149.24 (C-2), 168.25 (C-4). HRMS (ESI-MS) for $C_{11}H_{13}BrN_5O_4$ $[M+H]^+$ found, 358.0119; calcd, 358.0145.

3′-Deoxy-3′-(4-phenyl-1,2,3-triazol-1-yl)-β-(*E*)-5-(2-bromovinyl)-2′-deoxyuridine (14a). The reaction of compound **13** (64 mg, 0.18 mmol) with phenylacetylene (39 μL, 0.36 mmol) was performed as described in the general procedure for the synthesis of 4″-substituted 3′-deoxy-3′-(1,2,3-triazol-1-yl)- β-D-thymidine derivatives. Compound **14a** was obtained as a white solid in 6% yield (5 mg). ^{1}H NMR (300 MHz, DMSO-d_6): δ 2.73−2.80 (1H, m, H-2′a), 2.86−2.95 (1H, m, H-2′b), 3.66−3.70 (1H, m, H-5′a), 3.76−3.80 (1H, m, H-5′b), 4.32−4.34 (1H, m, H-4′), 5.34−5.48 (2H, m, 5′−OH and H-3′), 6.42 (1H, app t, J = 6.9 Hz, H-1′), 6.90 (1H, d, J = 13.2 Hz, bromovinyl), 7.28 (1H, d, J = 13.5 Hz, bromovinyl), 7.33−7.38 (1H, m, Ph), 7.44−7.50 (2H, m, Ph), 7.85 (2H, d, J = 5.1 Hz, Ph), 8.25 (1H, s, H-6), 8.77 (1H, s, H-5″). ^{13}C NMR (75 MHz, DMSO-d_6): δ 39.95 (C-2′), 55.47 (C-5′), 63.77 (C-3′), 84.66 (C-1′), 84.80 (C-4′), 108.00 (C-5), 109.92 (bromovinyl), 122.28 (C-5″), 126.89 (Ph), 129.77 (bromovinyl), 130.87, 131.58, and 133.20 (Ph), 139.02 (C-6), 144.25 (C-4″), 148.71 (C-2), 160.16 (C-4). HRMS (ESI-MS) for $C_{19}H_{19}BrN_5O_4$ $[M+H]^+$ found, 460.0637; calcd, 460.0615. Anal. ($C_{19}H_{18}BrN_5O_4$) C, H, N; C calcd, 49.58; found, 48.92.

3′-(4-Chlorophenyl-1,2,3-triazol-1-yl)-3′-deoxy-β-(*E*)-5-(2-bromovinyl)-2′-deoxyuridine (14b). The reaction of compound **13** (69 mg, 0.19 mmol) with 1-chloro-4-ethynylbenzene (52 mg, 0.38 mmol) was performed as described in the general procedure for the synthesis of 4″-substituted 3′-deoxy-3′-(1,2,3-triazol-1-yl)-β-D-thymidine derivatives, affording compound **14b** (6 mg) in a 6% yield. ^{1}H NMR (300 MHz, DMSO-d_6): δ 2.73−2.80 (1H, m, H-2′a), 2.85−2.94 (1H, m, H-2′b), 3.64−3.71 (1H, m, H-5′a), 3.75−3.81 (1H, m, H-5′b), 4.32−4.35 (1H, m, H-4′), 5.36−5.46 (2H, m, 5′-OH and H-3′), 6.41 (1H, app t, J = 6.9 Hz, H-1′), 6.89 (1H, d, J = 13.5 Hz, bromovinyl), 7.28 (1H, d, J = 13.5 Hz, bromovinyl), 7.52−7.56 (2H, m, Ph), 7.86−7.90 (2H, m, Ph), 8.21 (1H, s, H-6), 8.82 (1H, s, H-5″), 11.65 (1H, s, 3-NH). ^{13}C NMR (75 MHz, DMSO-d_6): δ 37.18 (C-2′), 55.73 (C-5′), 61.79 (C-3′), 84.59 (C-1′), 84.83 (C-4′), 107.44 (C-5), 109.90 (bromovinyl), 121.37 (C-5″), 126.89, 129.06, and 129.47 (4-chlorophenyl), 129.83 (bromovinyl), 132.461 (4-chlorophenyl), 139.54 (C-6), 145.51 (C-4″), 149.32 (C-2), 160.16 (C-4). HRMS (ESI-MS) for $C_{19}H_{18}BrClN_5O_4$ $[M+H]^+$ found, 494.0219; calcd, 494.0225. Anal. ($C_{19}H_{17}BrClN_5O_4$) C, H, N.

1-(3′-Deoxy-5′-*O*-triphenylmethyl-β-D-thymidin-3′-yl)-3-(4-chloro-3-(trifluoromethyl)-phenyl)-thiourea (15). To a suspension of 3′-amino-3′-deoxy-5′-*O*-triphenylmethyl-β-D-thymidine (2.36 g, 4.88) in DMF (44 mL) was added 4-chloro-3-(trifluoromethyl)-phenylisothiocyanate (1.0 mL, 6.35 mmol) in 58 mL of DMF at 0 °C. The reaction was stirred at room temperature for 3 h. The solvent was evaporated to dryness and the residue purified by column chromatography (CH_2Cl_2/MeOH 97:3). affording thiourea **15** as a white foam (3.44 g, 98%). ^{1}H NMR (300 MHz, DMSO-d_6): δ 1.46 (3H, d, J = 0.9 Hz, 5-CH_3), 2.26−2.34 (1H, m, H-2′a), 2.48−2.58 (1H, m, H-2′b), 3.18 (2H, d, J = 4.8 Hz, H-5′a and H-5′b), 4.07−4.12 (1H, m, H-4′), 5.21 (1H, app br s, H-3′), 6.28 (1H, app t, J = 6.6 Hz, H-1′), 7.24−7.44 (15H, m, Tr), 7.60−7.71 (3H, m, subs Ph), 8.03 (1H, s, H-6), 8.62 (1H, d, J = 6.3 Hz, 3′-NH), 9.84 (1H, s, N′H), 11.37 (1H, s, 3-NH). ^{13}C NMR (75 MHz, DMSO-d_6): δ 12.45 (5-CH_3), 37.52 (C-2′), 54.98 (C-5′), 64.69 (C-3′), 83.67 (C-1′), 84.31 (C-4′), 87.20 (Tr), 110.36 (C-5), 121.57 (CF_3), 125.19 (subs Ph), 126.78, 127.19, 127.59, 127.85, 128.40, 128.65, 128.80, and 128.99 (subs Ph and Tr), 132.37 and 136.24 (subs Ph), 139.71 (C-6), 144.13 (Tr), 151.06 (C-2), 164.35 (C-4), 181.32 (C=S). HRMS (ESI-MS) for $C_{37}H_{32}ClF_3N_4NaO_4S$ $[M+Na]^+$ found, 743.1677; calcd, 743.1675. Anal. ($C_{37}H_{32}ClF_3N_4O_4S$) C, H, N.

Experimental Assays. Radiochemicals. The radiolabeled substrate [CH_3-^{3}H]dThd (70 Ci/mmol) was obtained from Moravek Biochemicals (Brea, CA).

Thymidine Kinase Assay Using [CH_3-^{3}H]dThd as the Natural Substrate. The activity of recombinant thymidine kinase 1 (TK-1), TK-2, herpes simplex virus-1 (HSV-1) TK, varicella zoster virus (VZV) TK, and the multifunctional deoxynucleoside kinase (dNK) of *Drosophila melanogaster* and the 50% inhibitory concentration of the test compounds were assayed in a 50 μL reaction mixture containing 50 mM Tris/HCl, pH 8.0, 2.5 mM $MgCl_2$, 10 mM dithiothreitol, 0.5 mM CHAPS, 3 mg/mL bovine serum albumin, 2.5 mM ATP, 1 μM [methyl-^{3}H]dThd, and enzyme. The samples were incubated at 37 °C for 30 min in the presence or absence of different concentrations (5-fold dilutions) of the test compounds. At this time point, the enzyme reaction still proceeded linearly. Aliquots of 45 μL of the reaction mixtures were spotted on Whatman DE-81 filter paper disks (Whatman, Clifton, NJ). The filters were washed three times for 5 min each in 1 mM ammonium formate, once for 1 min in water, and once for 5 min in ethanol. The radioactivity was determined by scintillation counting.

To determine the K_m (for dThd or ATP) and K_i values (for the inhibitors), varying concentrations of dThd (ranging between 0.4 and 5 μM) were used at saturating concentrations of ATP (2.5 mM) or varying concentrations of ATP (ranging between 5 and 100 μM) at saturating concentrations of dThd (20 μM). The kinetic values were derived from Lineweaver−Burk plots.

Cytostatic Assay. Human osteosarcoma cells (OST TK-) that had been transduced by the *Drosophila melanogaster* deoxynucleoside kinase (Dm dNK) gene were seeded in 48-well plates at 20000 cells/1 mL well in DMEM supplemented with 10% fetal calf serum, 10 mM HEPES, 1 mM Na pyruvate, and 2 mM L-glutamine. The cells were incubated at 37 °C in the presence of 10 or 4 μM compound **14b**. One day later, serial dilutions of (*E*)-5-(2-bromovinyl)-2′-deoxyuridine (BVDU) and 5-fluoro-2′-deoxyuridine (5FdUrd) were added to the cell cultures. At day 4, cell number was counted using a Coulter particle counter model Z1, enabling the calculation of the 50% inhibitory concentrations of BVDU and 5FdUrd in the presence or absence of compound **14b**.

Molecular Modeling. The geometry of **8f**, modeled using as a template the AZT molecule found complexed to Dm-DNK in PDB entry 2JJ8, was optimized using the B3LYP method and a 6-31G(d) basis set, as implemented in the ab initio program Gaussian 03.[27] A reaction coordinate was performed to identify the two minima around the sugar−triazole bond, and electrostatic potential-derived (ESP) point charges were derived using the RESP methodology.[28] The thymine ring of compound **8f** was manually docked into the substrate-binding site of the previously reported[11] homology-based model of human TK-2 in complex with ATP and Mg^{2+}, and the two alternative locations for the phenyl triazole substituent were explored. Energy refinement of the resulting complexes and subsequent molecular dynamics simulations were carried out essentially as described[11] using the AMBER 10.0 suite of programs.[29] Bonded parameters for **8f** were automatically assigned using the general AMBER force field (GAFF) for organic molecules.[30] The molecular system consisting of human TK-2, ATP^{4-}, Mg^{2+}, and **8f** was immersed in a truncated octahedron of ∼6000 TIP3P water

molecules[31] and neutralized by addition of 5 sodium ions.[32] Periodic boundary conditions were applied and electrostatic interactions were treated using the smooth particle mesh Ewald method with a grid spacing of 1 Å. The cutoff distance for the nonbonded interactions was 9 Å, the SHAKE algorithm was applied to all bonds and an integration step of 2.0 fs was used. First, solvent molecules and counterions were relaxed by energy minimization and allowed to redistribute around the positionally restrained enzyme−inhibitor complex (25 kcal·mol^{-1}·Å^{-2}) during 50 ps of molecular dynamics at constant temperature (300 K) and pressure (1 atm). These initial harmonic restraints were gradually reduced until they were completely removed, and the complex was simulated for 10.0 ns in the absence of any restraints. After this time, the system was progressively cooled down from 300 to 273 K over 1.2 ns and subjected to energy minimzation. The computer graphics program PyMOL[33] was employed for visualization of structures and trajectories.

Acknowledgment. We thank the UGent Research Fund (BOF, Ghent University), the Fund for Scientific Research-Flanders (F.W.O.-Vlaanderen) for funding and the Institute for the Promotion of Innovation by Science and Technology in Flanders (IWT) for providing a scholarships to SVP Financial support to F.G. from Comisión Interministerial de Ciencia y Tecnología (SAF2006-12713-C02-02) and Comunidad de Madrid (S-BIO/0214/2006) is gratefully acknowledged.

Supporting Information Available: Multiple sequence alignment (ClustalW 2.0.10) and numbering of human TK-2 and related kinases; elemental analysis results of final compounds; cytotoxicity data of final compounds. This material is available free of charge via the Internet at http://pubs.acs.org.

References

(1) Eriksson, S.; Munch-Petersen, B.; Johansson, K.; Eklund, H. Structure and function of cellular deoxyribonucleoside kinases. *Cell. Mol. Life Sci.* **2002**, *59*, 1327–1346.
(2) Al-Madhoun, A. S.; Tjarks, W.; Eriksson, S. The role of thymidine kinases in the activation of pyrimidine nucleoside analogs. *Mini Rev. Med. Chem.* **2004**, *4*, 341–350.
(3) Saada, A.; Shaag, A.; Mandel, H.; Nevo, Y.; Eriksson, S.; Elpeleg, O. Mutant mitochondrial thymidine kinase in mitochondrial DNA depletion myopathy. *Nat. Genet.* **2001**, *29*, 342–344.
(4) Lewis, W.; Dalakas, M. C. Mitochondrial toxicity of antiviral drugs. *Nat. Med.* **1995**, *1*, 417–422.
(5) Lewis, W.; Day, B. J.; Copeland, W. C. Mitochondrial toxicity of NRTI antiviral drugs: An integrated cellular perspective. *Nature Rev. Drug Discovery* **2003**, *2*, 812–822.
(6) Balzarini, J.; Zhu, C. Y.; De Clercq, E.; Pérez-Pérez, M. J.; Chamorro, C.; Camarasa, M. J.; Karlsson, A. Novel ribofuranosylnucleoside lead compounds for potent and selective inhibitors of mitochondrial thymidine kinase-2. *Biochem. J.* **2000**, *351*, 167–171.
(7) Kierdaszuk, B.; Krawiec, K.; Kazimierczuk, Z.; Jacobsson, U.; Johansson, N. G.; Munch-Petersen, B.; Eriksson, S.; Shugar, D. Substrate/inhibitor properties of human deoxycytidine kinase (dCK) and thymidine kinase (TK1 and TK2) towards the sugar moiety of nucleosides, including *O′*-alkyl analogues. *Nucleosides, Nucleotides Nucleic Acids* **1999**, *18*, 1883–1903.
(8) Balzarini, J.; Degrève, B.; Zhu, C. Y.; Durini, E.; Porcu, L.; De Clercq, E.; Karlsson, A.; Manfredini, S. 2′-*O*-Acyl/alkyl-substituted arabinosyl nucleosides as inhibitor of human mitochondrial thymidine kinase. *Biochem. Pharmacol.* **2001**, *61*, 727–732.
(9) Pérez-Pérez, M. J.; Hernandez, A. I.; Priego, E. M.; Rodriguez-Barrios, F.; Gago, F.; Camarasa, M. J.; Balzarini, J. Mitochondrial thymidine kinase inhibitors. *Curr. Top. Med. Chem.* **2005**, *5*, 1205–1219.
(10) Hernandez, A. I.; Familiar, O.; Negri, A.; Rodriguez-Barrios, F.; Gago, F.; Karlsson, A.; Camarasa, M. J.; Balzarini, J.; Pérez-Pérez, M. J. N^1-substituted thymine derivatives as mitochondrial thymidine kinase (TK-2) inhibitors. *J. Med. Chem.* **2006**, *49*, 7766–7773.
(11) Balzarini, J.; Van Daele, I.; Negri, A.; Solaroli, N.; Karlsson, A.; Liekens, S.; Gago, F.; Van Calenbergh, S. Human mitochondrial thymidine kinase is selectively inhibited by 3′-thiourea derivatives of beta-thymidine: identification of residues crucial for both inhibition and catalytic activity. *Mol. Pharmacol.* **2009**, *75*, 1127–1136.
(12) Onderwater, R. C. A.; Commandeur, J. N. M.; Vermeulen, N. P. E. Comparative cytotoxicity of *N*-substituted *N′*-(4-imidazole-ethyl)-thiourea in precision-cut rat liver slices. *Toxicology* **2004**, *197*, 80–90.
(13) (a) Rostovtsev, V. V.; Green, L. G.; Fokin, V. V.; Sharpless, K. B. A stepwise Huisgen cycloaddition process: Copper(I)-catalyzed regioselective "ligation" of azides and terminal alkynes. *Angew. Chem., Int. Ed.* **2002**, *41*, 2596–2599. (b) Tornøe, C. W.; Christensen, C.; Meldal, M. Peptidotriazoles on solid phase: [1,2,3]-triazoles by regiospecific copper(I)-catalyzed 1,3-dipolar cycloaddition of terminal alkynes to azides. *J. Org. Chem.* **2002**, *67*, 3057–3064.
(14) Tron, G. C.; Pirali, T.; Billington, R. A.; Canonico, P. L.; Sorba, G.; Genazzani, A. A. Click chemistry reactions in medicinal chemistry: applications of the 1,3-dipolar cycloaddition between azides and alkynes. *Med. Res. Rev.* **2008**, *28*, 278–308.
(15) (a) Seo, T. S.; Li, Z.; Ruparel, H.; Ju, J. Click chemistry to construct fluorescent oligonucleotides for DNA sequencing. *J. Org. Chem.* **2003**, *68*, 609–612. (b) Lee, L. V.; Mitchell, M. L.; Huang, S. J.; Fokin, V. V.; Sharpless, K. B.; Wong, C. H. A potent and highly selective inhibitor of human α-1,3-fucosyltransferase via click chemistry. *J. Am. Chem. Soc.* **2003**, *125*, 9588–9589. (c) Gierlich, J.; Burley, G. A.; Gramlich, P. M. E.; Hammond, D. M.; Carell, T. Click chemistry as a reliable method for the high-density postsynthetic functionalization of alkyne-modified DNA. *Org. Lett.* **2006**, *8*, 3639–3642. (d) Kosiova, I.; Kovackova, S.; Kois, P. Synthesis of coumarin−nucleoside conjugates via Huisgen 1,3-dipolar cycloaddition. *Tetrahedron* **2007**, *63*, 312–320. (e) Seela, F.; Sirivolu, V. R. Nucleosides and oligonucleotides with diynyl side chains: Base pairing and functionalization of 2′-deoxyuridine derivatives by the copper(I)-catalyzed alkyne-azide "click" cycloaddition. *Helv. Chim. Acta* **2007**, *90*, 535–552. (f) Jatsch, A.; Kopyshev, A.; Mena-Osteritz, E.; Baeuerle, P. Self-organizing oligothiophene-nucleoside conjugates: versatile synthesis via "click"-chemistry. *Org. Lett.* **2008**, *10*, 961–964.
(16) (a) Cosyn, L.; Palaniappan, K. K.; Kim, S.-K.; Duong, H. T.; Gao, Z. G.; Jacobson, K. A.; Van Calenbergh, S. 2-Triazole-substituted adenosines: a new class of selective A(3) adenosine receptor agonists, partial agonists, and antagonists. *J. Med. Chem.* **2006**, *49*, 7373–7383. (b) Xia, Y.; Li, W.; Qu, F.; Fan, Z.; Liu, X.; Berro, C.; Rauzy, E.; Peng, L. Synthesis of bitriazolyl nucleosides and unexpectedly different reactivity of azidotriazole nucleoside isomers in the Huisgen reaction. *Org. Biomol. Chem.* **2007**, *5*, 1695–1701. (c) Li, L.; Lin, B.; Yang, Z.; Zhang, L.; Zhang, L. A concise route for the preparation of nucleobase-simplified cADPR mimics by click chemistry. *Tetrahedron Lett.* **2008**, *49*, 4491–4493.
(17) (a) Tourirte, M.; Oulih, T.; Lazrek, H. B.; Barascut, J. L.; Imbach, J. L.; Almasoudi, N. A. Synthesis of 3′-deoxy-3′-[4-(pyrimidin-1-yl)methyl-1,2,3-triazol-1-yl]thymidine via 1,3-dipolar cycloaddition. *Nucleosides, Nucleotides Nucleic Acids* **2003**, *22*, 1985–1993. (b) Skarpos, H.; Osipov, S. N.; Vorob'eva, D. V.; Odinets, I. L.; Lork, E.; Roschenthaler, G.-V. Synthesis of functionalized bisphosphonates via click chemistry. *Org. Biomol. Chem.* **2007**, *5*, 2361–2367. (c) Broggi, J.; Diez-Gonzalez, S.; Petersen, J. L.; Berteina-Raboin, S.; Nolan, S. P.; Agrofoglio, L. A. Study of copper(I) catalysts for the synthesis of carbanucleosides via azide-alkyne 1,3-dipolar cycloaddition. *Synthesis* **2008**, 141–148.
(18) (a) Kumar, R.; El-Sagheer, A.; Tumpane, J.; Lincoln, P.; Wilhelmsson, L. M.; Brown, T. Template-directed oligonucleotide strand ligation, covalent intramolecular DNA circularization and catenation using click chemistry. *J. Am. Chem. Soc.* **2007**, *129*, 6859–6864. (b) Lucas, R.; Neto, V.; Bouazza, A. H.; Zerrouki, R.; Granet, R.; Krausz, P.; Champavier, Y. Microwave-assisted synthesis of a triazole-linked 3′-5′ dithymidine using click chemistry. *Tetrahedron Lett.* **2008**, *49*, 1004–1007.
(19) Amblard, F.; Cho, J. H.; Schinazi, R. F. Cu(I)-catalyzed Huisgen azide-alkyne 1,3-dipolar cycloaddition reaction in nucleoside, nucleotide, and oligonucleotide chemistry. *Chem. Rev.* **2009**, *109*, 4207–4220.
(20) Whiting, M.; Muldoon, J.; Lin, Y. C.; Silverman, S. M.; Lindstrom, W.; Olson, A. J.; Kolb, H. C.; Finn, M. G.; Sharpless, K. B.; Elder, J. H.; Fokin, V. V. Inhibitors of HIV-1 protease by using in situ click chemistry. *Angew. Chem., Int. Ed.* **2006**, *45*, 1435–1439.
(21) Bourne, Y.; Kolb, H. C.; Radic, Z.; Sharpless, K. B.; Taylor, P.; Marchot, P. Freeze-frame inhibitor captures acetylcholinesterase in a unique conformation. *Proc. Natl. Acad. Sci. U.S.A.* **2004**, *101*, 1449–1454.
(22) Wigerinck, P.; Van Aerschot, A.; Claes, P.; Balzarini, J.; De Clercq, E.; Herdewijn, P. 3′-(1,2,3-Triazol-1-yl)-2′,3′-dideoxythymidine and 3′-(1,2,3-triazol-1-yl)-2′,3′-dideoxyuridine. *J. Heterocycl. Chem.* **1989**, *26*, 1635–1642.
(23) Huisgen, R. In 1,3-Dipolar Cycloaddition Chemistry; Padwa, A., Ed.; Wiley: New York, 1984; Vol. 1, pp 1−176.

(24) Zhang, L.; Chen, X.; Xue, P.; Sun, H. H. Y.; Williams, I. D.; Sharpless, K. B.; Fokin, V. V.; Jia, G. Ruthenium-Catalyzed Cycloaddition of Alkynes and Organic Azides. *J. Am. Chem. Soc*. **2005**, *127*, 15998–15999.
(25) Mikkelsen, N. E.; Munh-Petersen, B.; Eklund, H. Structural studies of nucleoside analog and feedback inhibitor binding to Drosophila melanogaster multisubstrate deoxyribonucleoside kinase. *FEBS J*. **2008**, *275*, 2151–2160.
(26) Egeblad-Welin, L.; Sonntag, Y.; Eklund, H.; Munch-Petersen, B. Functional studies of active-site mutants from *Drosophila melanogaster* deoxyribonucleoside kinase. Investigations of the putative catalytic glutamate−arginine pair and of residues responsible for substrate specificity. *FEBS J*. **2007**, *274*, 1542–51.
(27) Frisch, M. J.; Trucks, G. W.; Schlegel, H. B.; Scuseria, G. E.; Robb, M. A.; Cheeseman, J. R.; Montgomery, Jr., J. A.; Vreven, T.; Kudin, K. N.; Burant, J. C.; Millam, J. M.; Iyengar, S. S.; Tomasi, J.; Barone, V.; Mennucci, B.; Cossi, M.; Scalmani, G.; Rega, N.; Petersson, G. A.; Nakatsuji, H.; Hada, M.; Ehara, M.; Toyota, K.; Fukuda, R.; Hasegawa, J.; Ishida, M.; Nakajima, T.; Honda, Y.; Kitao, O.; Nakai, H.; Klene, M.; Li, X.; Knox, J. E.; Hratchian, H. P.; Cross, J. B.; Bakken, V.; Adamo, C.; Jaramillo, J.; Gomperts, R.; Stratmann, R. E.; Yazyev, O.; Austin, A. J.; Cammi, R.; Pomelli, C.; Ochterski, J. W.; Ayala, P. Y.; Morokuma, K.; Voth, G. A.; Salvador, P.; Dannenberg, J. J.; Zakrzewski, V. G.; Dapprich, S.; Daniels, A. D.; Strain, M. C.; Farkas, O.; Malick, D. K.; Rabuck, A. D.; Raghavachari, K.; Foresman, J. B.; Ortiz, J. V.; Cui, Q.; Baboul, A. G.; Clifford, S.; Cioslowski, J.; Stefanov, B. B.; Liu, G.; Liashenko, A.; Piskorz, P.; Komaromi, I.; Martin, R. L.; Fox, D. J.; Keith, T.; Al-Laham, M. A.; Peng, C. Y.; Nanayakkara, A.; Challacombe, M.; Gill, P. M. W.; Johnson, B.; Chen, W.; Wong, M. W.; Gonzalez, C.; Pople, J. A. *Gaussian 03*, revision B.04; Gaussian, Inc.: Wallingford, CT, 2004.
(28) Bayly, C. I.; Cieplak, P.; Cornell, W. D.; Kollman, P. A. A well-behaved electrostatic potential based method using charge-restraints for deriving charges: The RESP model. *J. Phys. Chem*. **1993**, *97*, 10269–10280.
(29) Case, D. A.; Darden, T. A.: Cheatham, T. E. III; Simmerling, C. L.; Wang, J.; Duke, R. E.; Luo, R.; Crowley, M.; Walker, R. C.; Zhang, W.; Merz, K. M.; Wang, B.; Hayik, S.; Roitberg, A.; Seabra, G.; Kolossváry, I.; Wong, K. F.; Paesani, F.; Vanicek, J.; Wu, X.; Brozell, S. R.; Steinbrecher, T.; Gohlke, H.; Yang, L.; Tan, C.; Mongan, J.; Hornak, V.; Cui, G.; Mathews, D. H.; Seetin, M. G.; Sagui, C.; Babin, V. Kollman, P. A. *AMBER 10*; University of California: San Francisco, 2008.
(30) Wang, J.; Wolf, R. M.; Caldwell, J. W.; Kollman, P. A.; Case, D. A. Development and testing of a general amber force field. *J. Comput. Chem*. **2004**, *25*, 1157–1174.
(31) Jorgensen, W. L.; Chandrasekhar, J.; Madura, J. D.; Impey, R. W.; Klein, M. L. Comparison of simple potential functions for simulating liquid water. *J. Chem. Phys*. **1983**, *79*, 926–935.
(32) Aqvist, J. Ion−water interaction potentials derived from free energy perturbation simulations. *J. Phys. Chem*. **1990**, *94*, 8021–8024.
(33) De Lano, W. *PyMOL* version 0.99; DeLano Scientific LLC: Palo Alto, CA, **2006**; http://www.pymol.org/.